

A FORMABILITY OF TWO COPPER-BEARING, COLD ROLLED, BOX ANNEALED AND TEMPER ROLLED EXTRA-DEEP DRAWING LOW CARBON ALUMINIUM-KILLED STEEL SHEETS OF NAGARJUNA STEEL LIMITED (PRIVATE, ANDHRA), AND A COMPARISON WITH THAT OF A TYPICAL STEEL SHEETS MADE BY BOKARO STEEL PLANT (STEEL AUTHORITY OF INDIA LIMITED, MINISTRY OF STEEL, GOVERNMENT OF INDIA)

A. KANNI RAJ

*Professor, School of Basic Sciences, Vel Tech Rangarajan Dr. Sagunthala
R&D Institute of Science & Technology, Chennai, Tamil Nadu, India*

ABSTRACT

This market-driven research publication is on the formability of two extra-deep drawing (EDD) steels in whose manufacture scrap addition is present and their chemistry may in turn show the presence of residual copper. It is known that the heat treatment response is significantly affected by the presence of copper. The present study was undertaken to evaluate the formability of two copper-bearing EDD steel sheets (0.07%Cu and 0.13%Cu). With the help of specially fabricated punch-die set up, stretching experiments were performed and in turn forming limit diagram (FLD) was plotted. Preliminary tests assess microstructural features, their behaviour in tension and formability parameters were also performed on both EDD sheets. It has been seen that both the 0.07%Cu and the 0.13%Cu EDD steel sheets displayed poor deep-drawability compared to 0.01%Cu EDD steel, mainly because of their low average plastic strain ratio (\bar{r}). The lower \bar{r} value (and as a consequences the reduced deep-drawability, especially, in the extra-deep drawing region) observed in the 0.07%Cu and 0.13%Cu EDD steel sheets could be due to poor processing, eg., use of a higher heating rate and reduced annealing time. TEM studies revealed no evidence for Cu precipitation in both the 0.07%Cu and 0.13%Cu EDD steels. Intensities of {111} texture components are low and in turn these heats show low formability.

KEYWORDS: *Formability, Forming Limit Diagram, Copper-Bearing Edd Steel, Extra-Deep Drawing, Strain Hardening Coefficient, Normal Anisotropy & Strain Distribution*

Received: Dec 13, 2018; **Accepted:** Jan 03, 2019; **Published:** Jan 24, 2019; **Paper Id.:** IJMPERDFEB201954

INTRODUCTION

Complex stampings are required for today automotive and various other industries. Such stampings are now developed with the aid of data obtained from laboratory experiments that enables the press formability of sheet metals to be reliably predicted [Kanniraj et al. 1998]. Hence, evaluation of formability of sheet steels helps in high quality stampings manufacture. By fixing variables involved in design by the way of fixed punch-die assembly, formability tests are done to identify influencing variables [Singh et al. 1994]. However, in shop floor, the process variables are optimized to yield maximum production rates at minimum cost and therefore, the

maximum exploitation of material ductility is greatly dependent upon the material properties. The press forming involves a quite high number of variables and shows a complicated interaction among them. Assessment of formability imitating press work condition is tough with any single parameter. Although the question for such a parameter has proved to be elusive till date, research efforts in that direction remain unremitting [Kanniraj. 2010].

Forming limit diagram (FLD) is an effective tool to evaluate the formability of sheet metals in various strain conditions. The information derived from the FLDs is very much useful for the sheet metal industries and end users. Because of its importance, research on such detailing is plentiful in literature both in experimentation and modelling [Zhang et al. (2018), Takalkar et al. (2015), Reddy.(2017), Hora et al. (2012), Srinivasan et al. (2014)]. Since the formability and FLD depend on any different factors and conditions of sheet metals, many experimental investigations also have been carried out. Steel is used in automotives to withstand the body weight under strong pressure of the requirements for fuel conservation, energy saving, and crash-worthiness. EDD steel is widely used in such applications. Extra-deep drawing (EDD) steels are the most widely used steel material today for automotive applications involving simple to complex stampings which require very high formability, mainly stretchability and drawability [Tisza et al. 2018]. Most of the automotive parts are made on EDD steel. Also, these steel sheets finds lot of applications, viz., households such as baths and sink units, refrigerator panels, many industrial components, modern building structures, etc. In the present work, formability of three heats of indigenously produced aluminium-killed EDD low carbon steel sheets has been characterized in terms of their microstructure, mechanical properties and forming limit diagram (FLD) [Reddy. (2017), Stoughton et al. (2012), Sivam et al. (2015), Goud et al. (2014)]. Sheets with a wide variation in copper content and same thickness were chosen for the present study. The principle aim has been to obtain a quantitative manner the effect of variation in formability and the corresponding texture level upon press formability. All the sheets were received in cold-rolled, box-annealed and temper-rolled condition. The copper-bearing EDD steel sheets of dimensions 500mmX500mmX1.25mm were received from the private limited steel plant (NSL Limited, Patancheru, Andhra Pradesh). The EDD steel for benchmarking purpose is taken from Indian public sector steel giant SAIL's Bokaro Steel Plant.

EXPERIMENTAL METHODS

Chemical Composition and Mechanical Properties

By an emission spectrometer known as Spectrovac (Model ARL 3460 metals analyser), steel chemistry was clearly understood and composition so obtained was tabulated. This spectrometer provides C, Mn, Al, Si, Cu, Sn, P and S composition minutely and accurately (given percentage of N and O are less accurate). With the help of the Leco gas analyser (present in IGCAR Kalpakkam), amount of nitrogen and oxygen present was exactly obtained and added to composition table. Optical metallographs (specimen made as per ASTM procedure) were taken in order to correlate micro structural features with mechanical properties. The two-dimensional grain size (d_0) was measured using the average linear intercept method at different magnifications. ASTM E8M full size specimens were used to obtain tensile properties, on a 400kN capacity Schenck closed-loop servo-hydraulic testing machine (Equipment Made in Germany). The standard tensile properties, viz., 0.2% yield stress (YS), ultimate tensile stress (UTS), uniform elongation (e_u), total elongation (e_f), strain hardening exponent (n) and strength coefficient (K) were determined from the load-elongation data obtained from the above testing. A constant crosshead speed of 1.0mm/min (corresponding to an initial strain rate of $5.56 \times 10^{-4} \text{ s}^{-1}$) was employed in all cases. Tested specimens contained three different orientations (length axis along 0° , 45° and 90° to sheet rolling direction) and averaged properties were evaluated. To account for experimental scatter, three samples used for each

$$X_{average} = \frac{X_0 + 2X_{45} + X_{90}}{4} \quad (1)$$

Where $X_{average}$ is the mean value of any property and the other suffixes denote the angle between tensile axis and sheet rolling direction. Strain rate sensitivity index (m), was calculated from the results of strain rate jump tests carried out on tensile specimens. The crosshead speed (strain rate) was suddenly raised when the specimen deformation was in uniform plastic strain region. The m value is calculated using Equation 2.

$$m = \frac{\ln\left(\frac{\sigma_2}{\sigma_1}\right)}{\ln\left(\frac{\dot{\epsilon}_2}{\dot{\epsilon}_1}\right)} = \frac{\ln\left(\frac{P_2}{P_1}\right)}{\ln\left(\frac{V_2}{V_1}\right)} \quad (2)$$

Where σ_1 and σ_2 are flow stresses at strain rates $\dot{\epsilon}_1$ and $\dot{\epsilon}_2$ respectively, and P_1 and P_2 are loads corresponding to crosshead speeds of V_1 and V_2 , respectively. Jump tests were also performed on ASTM E8M full size specimens. A strain rate jump of 11 times was used (initial strain rate before the jump was $5.56 \times 10^{-5} \text{ s}^{-1}$ and strain rate after the jump was $6.1 \times 10^{-4} \text{ s}^{-1}$). Average m value was evaluated from Equation 1. The Vickers hardness value of these three heats of EDD steels in the as-received conditions were measured. Erichsen cup depth values were also measured using the standard tester. The parameters n, \bar{r} and Δr used to primarily assess formability. In MS Excel software, by regression on true stress-true strain data, n values were calculated, obeying Hollomon equation (Equation 3).

$$\sigma = K \epsilon^n \quad (3)$$

Where σ is stress, ϵ the strain and K the strength coefficient. The value of n can also be obtained from the following three equations (Equations 4-6).

$$n = \epsilon_u \quad (4)$$

$$n = \frac{5}{10 + d_0^{-0.5}} \quad (5)$$

$$N = 0.28 - 0.2C - 0.25Mn - 0.044Si - 0.039Sn - 1.2N \quad (6)$$

Liu and Johnson method was used to get r values and in turn to calculate \bar{r} and Δr . In this method, specimen prepared as per ASTM E517, were incrementally deformed, by measuring major strain (ϵ_l) and minor strain (ϵ_w) at equal elongation intervals. The strains were measured in the gauge length (marked in the central portion of the specimen) [Kanniraj. 2010]. The r value was then evaluated from the slope the plot of ϵ_w versus ϵ_l using the Equation 7.

$$r = \frac{\epsilon_w}{\epsilon_t} = \frac{\epsilon_w}{\epsilon_l + \epsilon_w} \quad (7)$$

Where ϵ_w , ϵ_t and ϵ_l are strains in width, thickness and length direction of the specimens. The r value obtained by the above method is strain-independent and free from scatter. Tested specimens contained three different orientations, ie, specimen length axis along 0° , 45° and 90° to sheet rolling direction. The normal anisotropy or the average plastic strain ratio, \bar{r} and the planar anisotropy Δr was calculated using the standard formulae (Equations 8 and 9)

$$\bar{r} = \frac{r_0 + 2r_{45} + r_{90}}{2} \quad (8)$$

$$\Delta r = \frac{r_0 - 2r_{45} + r_{90}}{2} \quad (9)$$

where the subscripts 0, 45 and 90 indicate the orientation of the specimen axis with respect to the rolling direction.

Formability Testing and microstructural Analysis

FLD graph was plotted by Hecker's method. Accordingly to say, 5mm non-contacting grid circles were printed in sample sheets, sheets were then punch-stretched to failure or onset of localized necking, and strain was measured using a flexible scale. The grid pattern was etched on the samples using Systronics electrochemical etching equipment. Punch-stretching experiments were carried out on a 1000 kN (100 tonnes) capacity double-action Becker & van Hullen hydraulic press at a crosshead speed of 10mm/min (Press Made in Germany). With the help of specially designed and machined punch-die set up (made for 1.25mm thick sheet), stretching experiments were performed. A typical punch-die assembly used in the experiments as found in the literature [Kanniraj et al. 1998]. The sheet samples were subjected to different states of stain, i.e., biaxial tension, plain strain and compression-tension incorporated by blank width variation. The sample sizes were of 200mmX200mm, 200mmX175mm, 200mmX150mm, 200mmX125mm, 200mmX100mm, 200mmX75mm, 200mmX50mm and 200mmX25mm. Four numbers each of all eight blank samples helped to generate more data points. Tension tested grid marked sampled was used to generate data pertaining to extremely high minor strain region. Stretching was done till the onset of localized necking or till failure. The circles got transformed into ellipses after deformation. In each stretched-blank; few fractured, few safe and few necked ellipses, were marked for strain measurement. The major and minor diameters of the ellipses, using a transparent, flexible plastic scale, were plotted against each other by plotting the minor strain in abscissa and major strain in the ordinate. FLD curve was drawn as a line separating safe ellipse data points from necked or failed ellipse data points [Kanniraj. 2008]. In these experiments, accuracy of FLD curve is within $\pm 2\%$ strain. FLD line was obtained by a least square analysis using Microsoft EXCEL software and it follows the polynomial of the form (Equation 10) and standard error lines were also calculated (Equation 11).

$$Y_{1i} = a_0 + a_1 e_{2i} + a_2 e_{2i}^2 + \dots + a_x e_{2i}^x \quad (10)$$

Where Y_{1i} is the i^{th} estimated major strain, e_{2i} is the i^{th} experimental minor strain, X degree of polynomial providing best fit with least error, a 's are the polynomial coefficients.

$$\sigma_{error} = \sqrt{\frac{\sum_{i=1}^{i=N} (e_{1i} - Y_{1i})^2}{N}} \quad (11)$$

Where e_{1i} is the i^{th} experimental major strain, N the number of data points and σ_{error} is the standard error in the FLD line. Major and minor strain distribution plots along longitudinal axis of all blanks show different states of stress. Samples of fully deformed blanks with crack initiated or deformed to the onset of severe localized necking were only selected. Measured strains of all ellipses along the longitudinal axis were plotted against the centre distance from the centre of the blank. An ellipse centre from the centre of the blanks is called a pole. The pole in abscissa against major strains and minor strains in ordinate is called strain distribution profile. The plots are not shown to strict of a journal paper size upper limit constraint and a similar set of plots can be accessed in other journal papers written by the authors [Kanniraj et al. 1998]. Constraint factor f and error in f were evaluated using Equations 12 and 13 respectively, and plotted against true peak minor strain.

$$f = \frac{\varepsilon_{2peak} - \varepsilon_{2pole}}{\varepsilon_{1peak} - \varepsilon_{1pole}} \quad (12)$$

Where ε_{2pole} and ε_{1pole} are the values of the true minor and major strains at the pole respectively, and ε_{2peak} and ε_{1peak} are

$$\frac{df}{f} = \frac{d\varepsilon_{2peak} - d\varepsilon_{2pole}}{\varepsilon_{2peak} - \varepsilon_{2pole}} - \frac{d\varepsilon_{1peak} - d\varepsilon_{1pole}}{\varepsilon_{1peak} - \varepsilon_{1pole}} \quad (13)$$

Where $d\varepsilon$'s are variation in ε 's. The plots of $\varepsilon_2/\varepsilon_1$ ratio at a particular distance against blank widths have also been plotted. The specimens for TEM analysis were cut, polished by emery papers and finally thinned down using a twin jet electrochemical etching polisher with 15% perchloric acid in methyl alcohol as electrolyte. The TEM micrographs were taken using a Phillips scanning electron microscope with EDAX facility (model CM12). The TEM and EDAX analyses of the material in homogeneities (phases/precipitates) were evaluated. Siemens D500 X-ray computerized goniometer (Made in Germany) was used to analyse texture of 0.07% Cu EDD steel and to understand the deviation of its formability from regular EDD steel (Made in SAIL).

RESULTS AND DISCUSSIONS

Chemical Composition and Mechanical Properties

Table1 shows the steel chemistry of EDD sheets taken for analysis. The amount of carbon in the Cu-bearing steels were lower than 0.01%Cu EDD steel that is the desired carbon level for good drawability. Higher carbon content of 0.01%Cu EDD steel lowers \bar{r} . Also, high C% raises amount of cementite and lowers grain size. High \bar{r} values (>1.6) have been observed in case of the EDD steel sheets with carbon less than 0.05%. So, the Cu-bearing steels considered in the present studies are good, since the carbon content may not pose significant problem, any variation in their formability due to this. Mn content in 0.02-0.14% is good for drawability, as it stops stringer formation. High coiling temperature increases \bar{r} in rolling direction. They attributed this to the changes in the distribution of MnS inclusion and the precipitation of Al/N. But, in all the three heats of the study are higher than this range. The presence of aluminium up to 0.08% had no adverse effect on the mechanical properties. Aluminium content in all the heats is lower than this value. More importantly, it is the ratio of aluminium to nitrogen contents which affect the formability significantly. The desired ratio of aluminum to nitrogen is around 10. The solutes nitrogen and aluminium forms AlN and helps in {111} texture formation and thereby achieving high \bar{r} value. From earlier research, it was concluded that best \bar{r} value is associated with a steel chemistry bearing 0.0065-0.0095% nitrogen and 0.04-0.07% aluminium. All the heats are safe in this range and hence a favourable texture and a high \bar{r} value was expected and proved by X-ray diffraction studies [Kanniraj. 2010].

Table 1: Chemical Composition of the Three Aluminium-Killed Extra-Deep Drawing Low Carbon Steel Sheet

| Heat → | 0.01%Cu EDD steel | 0.07%Cu EDD steel | 0.13%Cu EDD steel |
|-----------|----------------------|----------------------|----------------------|
| C | 0.078 | 0.037 | 0.031 |
| Al | 0.053 | 0.028 | 0.041 |
| N | 0.032 | 0.045 | 0.059 |
| O | 0.055 | 0.045 | 0.059 |
| Mn | 0.370 | 0.182 | 0.181 |
| Cu | 0.01% | 0.07% | 0.13% |
| Fe | Balance | Balance | Balance |

Figures 1 and 2 show the optical micrographs. From micrograph by the linear intercept method, grain size was obtained are accurate to within $\pm 2\mu\text{m}$. The grain size is 8 (ASTM No) for the three heats. This grain size is good for deep

drawing applications. As expected, n and \bar{r} increases along with grain size. The \bar{r} and d of many AK EDD steels show an increasing trend with increasing annealing at high temperature till complete phase transformation. The effect of annealing temperature and hence d on the \bar{r} value of a Cu-bearing steel has been shown to be significant. Also, t_0/d_0 ratio 60-75 decides thickness strain. The highest thickness strain reported for a t_0/d_0 ratio in the range 60-75. This ratio lies in the range for both heats (0.07% Cu and 0.13% Cu EDD steels).

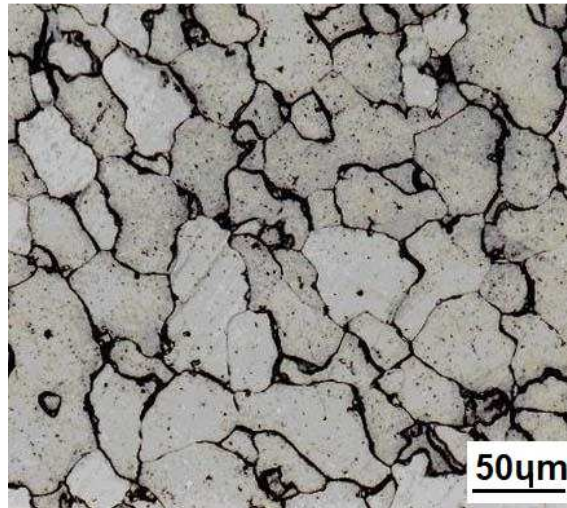


Figure 1: An Optical Micrograph of the 0.07% Cu EDD Steel Sheet. 5% Nital was used to Etch

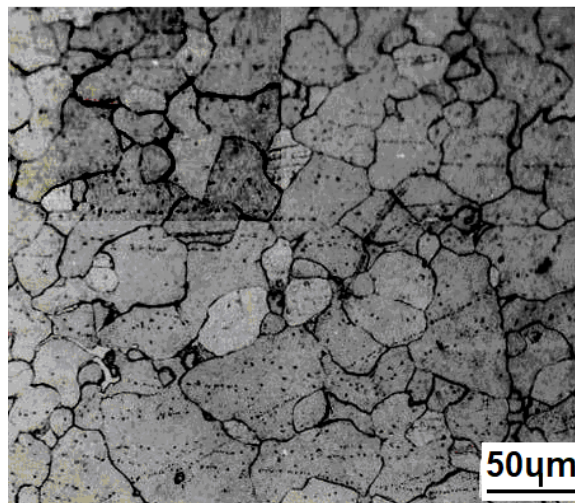


Figure 2: An Optical Micrograph of the 0.13% Cu EDD Steel Sheet. 5% Nital was used to Etch

The average values of mechanical properties are shown in Table 2. Cu-bearing EDD steels and the benchmark steel exhibited higher strength values and lower ductility. The n values are low compared to standard EDD steel and hence these steels showed poor stretch ability. The m values are very small and positive for all grades used in the present analysis. This is as expected for most of the common metals, ie, low sensitivity at room temperature. The hardness values (in Vicker's scale) of the three heats in the as-received condition are given in Table 2. The value lies in the range of 108-111 Hv, typical of deep-drawing steels. Erichsen cup depth values are also shown in Table 2. The values of all heats were comparable.

Table 2: Tensile Properties of the Three Aluminium-Killed Extra-Deep Drawing Low Carbon Steel Sheet

| Heat → | 0.01%Cu EDD steel | 0.07%Cu EDD Steel | 0.13%Cu EDD Steel |
|----------------|----------------------|----------------------|----------------------|
| YS (MPa) | 224 | 210 | 175 |
| UTS(MPa) | 303 | 306 | 300 |
| e _u | 26 | 30 | 31 |
| e _t | 39 | 41 | 41 |
| n | 0.21 | 0.22 | 0.25 |
| K (MPa) | 516 | 508 | 533 |
| m | 0.01 | 0.01 | 0.01 |
| Hv | 111 | 111 | 108 |
| Ev | 11 | 10.9 | 10.8 |

Figure 3 shows the flow curves of the Cu-bearing EDD steels. The curves are typical of EDD steels. A conventional indicator of formability, viz., the strain hardening exponent n is obtained from the regression of the Hollomon equation $\sigma = K\epsilon^n$ and is shown in Table 2. The n values obtained by all modes and the average plastic strain ratio, or normal anisotropy \bar{r} (determined using Liu and Johnson's technique), the product $n\bar{r}$ and Δr are enumerated in Table 4. The n value is in the range 0.21-0.25 indicating sufficiently good stretchability. With low $n\bar{r}$, 0.01%Cu EDD is expected to have low formability. As $n\bar{r}$ is high for 0.13%Cu EDD, it possesses good formability. High Δr is indicative of earing behaviour, and is noted in 0.13%Cu EDD steel. It is consistent with the fact that a sheet with high \bar{r} generally possesses high Δr also. It is to be noted that the ideal situation of high \bar{r} and low Δr is difficult to achieve under normal processing conditions [Singh et al. 1994].

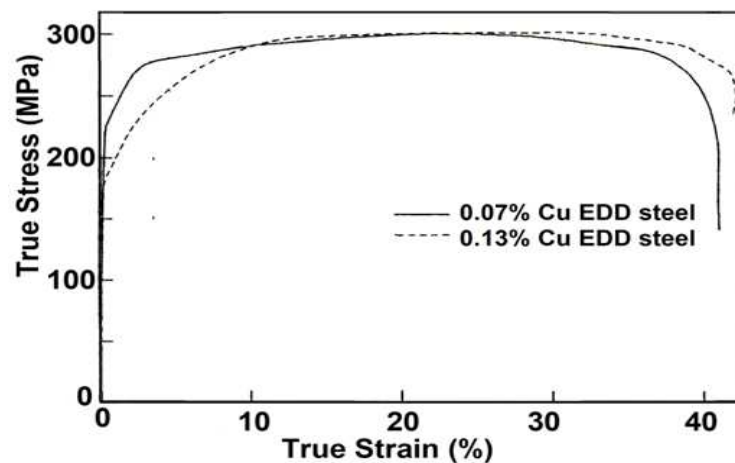


Figure 3: Room Temperature Flow Curves Of 0.07%Cu and 0.13%Cu EDD Steel Sheets

Table 3: Formability Parameters of the Three Aluminium-Killed Extra-Deep Drawing Low Carbon Steel Sheet

| Heat → | 0.01%Cu EDD steel | 0.07%Cu EDD steel | 0.13%Cu EDD steel |
|------------------|----------------------|----------------------|----------------------|
| n by Regression | 0.21 | 0.22 | 0.25 |
| n=e _u | 0.23 | 0.26 | 0.27 |
| n by Pickering | 0.16 | 0.16 | 0.15 |
| n by Morrison | 0.28 | 0.33 | 0.32 |
| r ₀ | 1.65 | 1.52 | 1.38 |
| r ₄₅ | 1.26 | 1.29 | 1.25 |
| r ₉₀ | 2.06 | 1.7 | 1.85 |

| Table 3 Contd., | | | |
|-----------------|-------|-------|-------|
| \bar{r} | 1.56 | 1.45 | 1.43 |
| Δr | 0.29 | 0.32 | 0.37 |
| $N\bar{r}$ | 0.328 | 0.319 | 0.358 |

Stretchability and n are directly proportional. Table 3 gives n values. The n values obtained by regression of Hollomon equation and empirical equation based on steel chemistry agrees well. This empirical equation is $n = 0.28 - 0.2[C] - 0.25[Mn] - 0.044[Si] - 0.039[Sn] - 1.2[N]$. The values obtained from the above equation are almost equal for all heats. This is mainly due to similar chemistry of all study heats. Clearly this empirical equation has very limited applicability. The relationship between n and grain size, d is also used to get n . The n values obtained based on the above equation are higher than those obtained from other three methods. However, only the values obtained from the regression analysis are used in all further discussions. Table 3 shows \bar{r} obtained from various methods. It can be observed that the \bar{r} value is higher for benchmark heat and indicating good drawability. The Cu-bearing EDD steels have low \bar{r} value indicating their inferior drawability. The \bar{r} values determined using Liu and Johnson's technique is strain independent and also normalizes any experimental scatter. These are indicative of high formability, especially drawability.

Formability Testing and microstructural Analysis

FLDs, evaluated experimentally for the Cu-bearing EDD steel sheets following Hecker's method, are shown in Figure 4. FLDs shows trend as expected from n , m , \bar{r} and Δr . The slopes of the FLD curves are tallying with \bar{r} values. Both Cu-bearing EDD steels show high limit strains. All heats have good stretchability while the only benchmark heat have excellent drawability. So, mechanical properties and microstructural features match with trends observed in limit strains to a large extent. But some features are difficult to explain. Though it is possible to correlate mechanical properties and microstructural features with forming limit strains, some degree of discrepancy in correlation may be due to a complicated interaction of process variables. So, comparative explanation without process variables analysis is tough. Deep drawability of both Cu-bearing steels was similar, but inferior when compared with that of the 0.01%Cu EDD steel. Deep drawability depends on normal anisotropy (\bar{r}) which in turn depends on the crystallographic texture. The texture formation is affected by the presence of copper. Thus, because of their lower \bar{r} value compared to 0.01% Cu EDD steel, the Cu-bearing steels showed poor deep drawability. Formability in/near plane strain forming of both the Cu-bearing EDD steels was better than that of 0.01%Cu EDD steel. Meanwhile, biaxial stretchability of 0.07%Cu EDD steel was slightly greater than 0.13%Cu EDD steel whilst that of 0.01%Cu EDD steel was still lower. The good stretchability associated with the Cu-bearing steels are due to the greater n value.

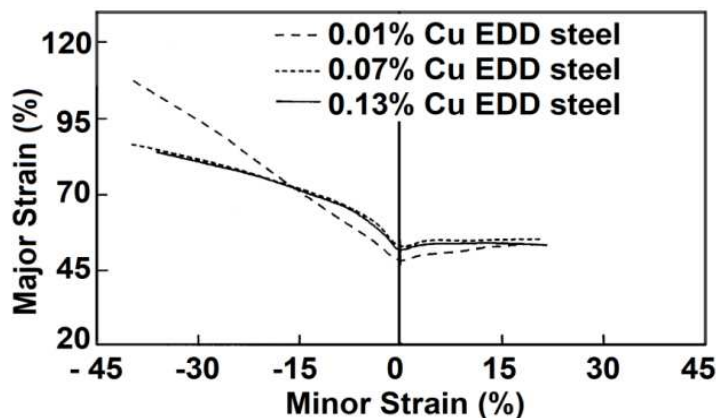


Figure 4: A Comparison of the Mean Forming Limit Curves of 0.01%Cu, 0.07%Cu and 0.13%Cu EDD Steel Sheets

Even with optimized tool geometry, strain gradients were present due to the presence of stress gradients caused by friction at the sheet/punch interface. Strain distribution profiles (not shown here, due to paper size upper limit) showed similar shapes for both Cu-bearing EDD steels. The profiles are asymmetric in the heights. This was because when a strain peak develops into a localized neck (due to chance variations in local sheet thickness and/or metallurgical inhomogeneity), the other peak ceased to grow further causing the observed asymmetry. Though plots not presented, the strain distribution plots were generated for all blank widths.

The special features of strain distribution profiles are enumerated below.

- Two peaks were obtained for all blank widths (200, 175, 150, 125, 100, 75, 50 and 25, sizes in mm).
- Blank widths 200, 175, 150 and 125mm fall in biaxial stretching category and show two positive peaks. Blank widths 100, 75, 50 and 25 mm, the minor strain progressively goes down and minor strain become negative due to lateral drawing-in. For low blank widths, the peaks are negative.
- Asymmetry in strain peaks on either side is due to fracture and in turn load action ceased in one side.
- Low blanks show peaks near die throat. Lateral drawing-in increases separation between peaks.
- Variation trend for the pole to peak against blank width is similar for all heats. A similar observation was made earlier in case of materials with \bar{r} value greater than unity.
- Mostly, strain ratio at failure is close to plain strain conforming to the usual behaviour of EDD steels.

Effect of n and \bar{r} on strain distribution characteristics are very strong and so few brief comments are included.

- Stretchability is strongly affected by n value and drawability by \bar{r} value
- Higher values of both n and \bar{r} shift the major strain peak towards the die.
- High n lowerd peak major strain, whilst high \bar{r} on contrary rise major strain peak value.
- Also, according to finite element calculations, the half width would increase with increase in both n and \bar{r} values.
- There is a decrease in maximum thickness strain with n/\bar{r} value.
- Polar thickness strain is almost independent of n but increases with decreasing \bar{r} value.

In view of the major and the minor strain gradients present due to friction, a constraint factor, f was determined. Also, error in f also determined. Figure 5 shows a plot of f against $\epsilon_{2\text{peak}}$ for the 0.07%Cu and 0.13%Cu EDD steels. The plot shows a comparison of the constraint factors of the two copper-bearing steels as a function of $\epsilon_{2\text{peak}}$. The plot of f is similar in the case of both steels (similar friction effects). The plots not shown here, the dependence of the major strain to the minor strain ratio on the blank width was plotted, at a fixed distance from the pole. In both the sheets, e_2/e_1 ratio decreased with increasing distance from the pole and in all cases the plots were sigmoidal. The curves lie in a narrow band at lower blank widths (below 125mm) but get separated at higher blank widths. It should be noted that beyond a certain width (in all cases 125mm) the entire draw bead would have made contact with the blank and there would be no further increase in the constraints or stretching force in the e_2 direction. Then (e_2/e_1) -blank width plots will flatten out. Literature data on the dependence of the e_2/e_1 on the blank width for a

typical EDD sheet steel showed a similar trend.

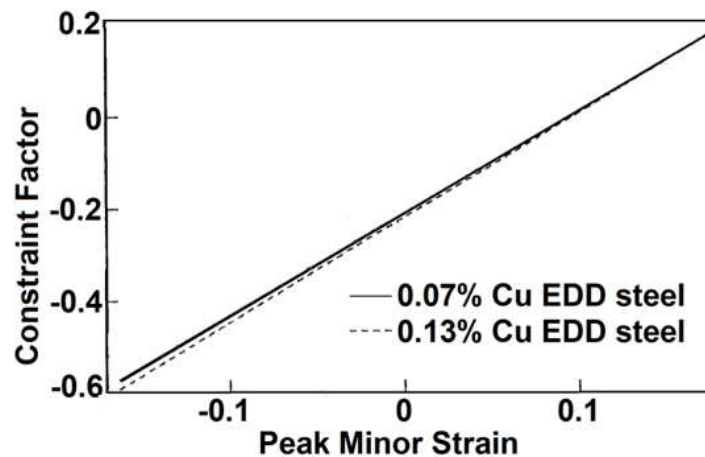
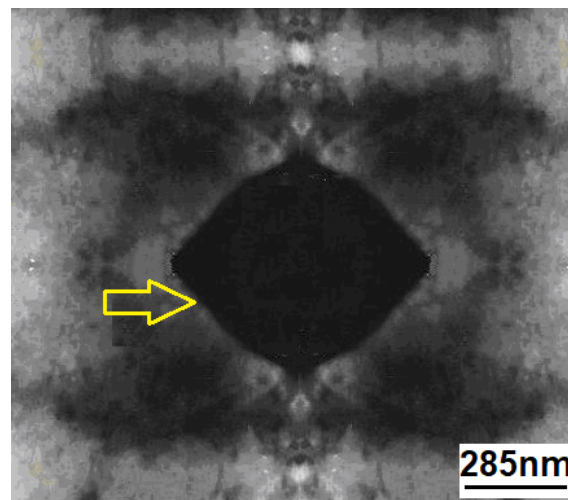


Figure 5: A Comparison of Constraint Factors in 0.07%Cu and 0.13%Cu EDD Steel Sheets

All these experimental observations clearly indicates that (a) the formability of both Cu-bearing steels is comparable, (b) the deep drawability of Cu-bearing steels is inferior to that of the 0.01%Cu EDD steel used as benchmark, (c) the 0.01%Cu EDD steel shows slightly inferior formability in the plane strain forming condition because of its low \bar{r} value, and (d) the variations in the mechanical properties of Cu-bearing steels with 0.01%Cu EDD steel is likely to be due to the variations in the control of the processing parameters and steel chemistry. The present investigation clearly shows that the Cu-bearing steels (0.07%Cu and 0.13%Cu EDD steels) have inferior deep drawability mainly because of their lower \bar{r} values compared to the usual EDD range. Annealing texture, which contains $\{111\}<110>$, $\{111\}<112>$ and $\{554\}<225>$ as major components, is responsible for obtaining high \bar{r} values and hence excellent deep drawability in EDD steels. During annealing at 973K, Al and N precipitate completely as AlN particles, which act as obstacles to grain growth and so prolonged annealing is required to obtain sufficiently large grains to improve ductility. Thus poor processing such as the use of a higher heating rate (30% higher) and reduced annealing time (40% lower) in the case of the Cu-bearing steels compared with 0.01%Cu EDD steel might have led to lower deep drawability. (Exact data on the processing parameters employed by the manufacturers of the Cu-bearing steels were not available. Deep drawability depends strongly on the processing parameters, eg., the finishing temperature, the coiling temperature, the amount of cold reduction, the characteristics of annealing, the skin passing, etc. The effects of these parameters can completely overshadow the effects of small variations in steel chemistry. So a proper control over the processing parameters appears to be more important if the steels are to prove successful in critical EDD applications. It should be checked by the manufacturers using similar processing routes if the forming failures reported is in more severe forming applications than in the cases where forming has been successful. The idea that the failure could be due to increased copper content in Cu-bearing steels is not borne out by the present study. However, it is conceivable that increasing the copper content in the steel may have an effect on texture development during annealing. But the copper addition up to 1.2% in deep drawing steels has facilitated the obtaining of strong $\{111\}$ -type texture and hence a higher \bar{r} value [Kanniraj. 2010]. Cu addition, on the other hand, diminished stretchability and resistance to strain ageing. The Cu-bearing steels used in the present investigation, however, showed better stretchability and practically no effect on the deep drawability with a change in the Cu level.

Figures 6 and 7 show TEM micrographs of 0.07%Cu EDD and 0.13% Cu EDD steels. Figure 8 shows an EDAX graph for 0.13% Cu EDD steel. The investigation on the four figures showed no evidence for copper precipitation. So, the

effect of residual copper on reducing the overall formability of both the Cu-bearing steels is ruled out. As analysed based on the effect of steel chemistry-in particular of copper-on the annealing behaviour and texture formation is beyond the scope of the present investigation. Pictorial representation of orientation distribution function components of 0.07% Cu EDD steel in $\Phi_2=45^\circ$ sections is shown in Figure 9. Intensities of $\{111\}$ texture components are low and in turn shows low f accounting for poor formability. Mostly improper processing such as low annealing time along with little influence of copper in texture development are major reasons for low formability of these steels. However, the suspicion of the industry that premature failure could have been due to the increased Cu content was not borne out fully by the present study. This point is to be further verified by more rigorous texture analysis, which will be carried out as a new research project.



**Figure 6: A TEM Picture of the 0.07% Cu EDD Steel Sheet.
A Fe-based Precipitate is Indicated by an Arrow**

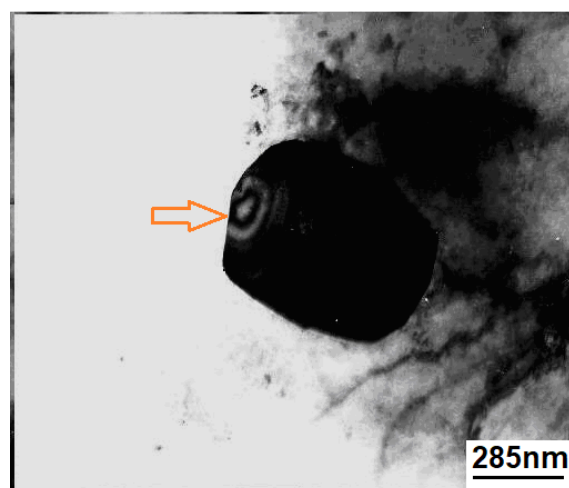


**Figure 7: A TEM Picture of the 0.13% Cu EDD Steel Sheet.
A Fe-Based Precipitate is Indicated by an Arrow**

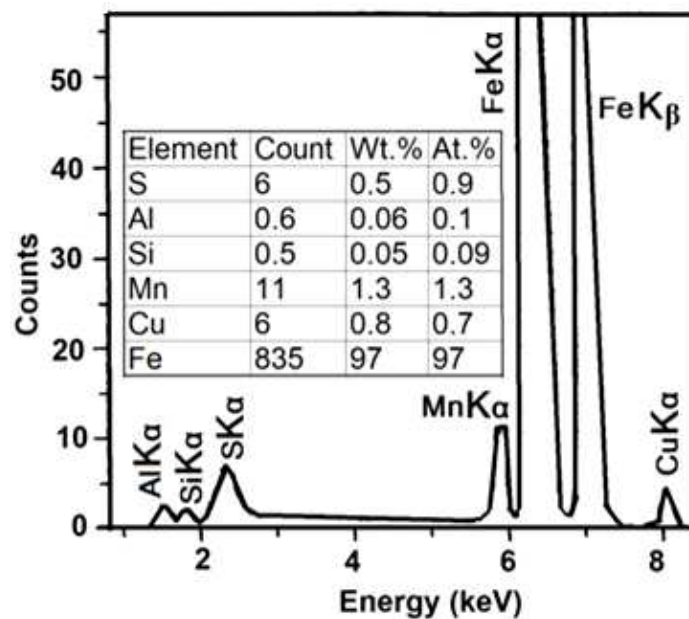


Figure 8: An EDAX Analysis of the Fe-Based Precipitate in 0.13% Cu EDD Steel Sheet. The Analysis was at the Centre of the Precipitate Shown by Arrow in Previous Figure

CONCLUSIONS

The major conclusions of the present study on Cu-bearing EDD low carbon steel sheets were as follows.

- Ductility (uniform and total elongations) of the 0.07%Cu and 0.13%Cu EDD steel sheets were greater than that of the 0.01%Cu EDD steel sheet.
- Uniform elongation and UTS/YS ratio paralleled the changes in strain hardening exponents.
- The Cu-bearing steels displayed poor deep drawability compared to benchmark (0.01%Cu EDD steel).
- The stretchability of the Cu-bearing EDD steel sheets were greater when compared with 0.01%Cu EDD steel sheet, mainly because of their low normal anisotropy.
- The lower \bar{r} value (and as a consequence the reduced drawability, especially, in the EDD region) observed in the Cu-bearing EDD steel sheets could be due to poor processing, eg., use of 30% higher heating rate and 40% lower annealing time.
- TEM studies revealed no evidence for Cu precipitation in both the Cu-bearing EDD steels.
- Intensities of $\{111\}$ texture components are low and in turn shows low f accounting for poor formability. Mostly improper processing such as low annealing time along with little influence of copper in texture development are major reasons for low formability of these steels.
- However, the suspicion of the industry that premature failure could have been due to the increased Cu content was not fully borne out by the present study. This point is to be further verified by more rigorous texture analysis.
- Strain distributions were similar in both the Cu-bearing EDD steel sheets.

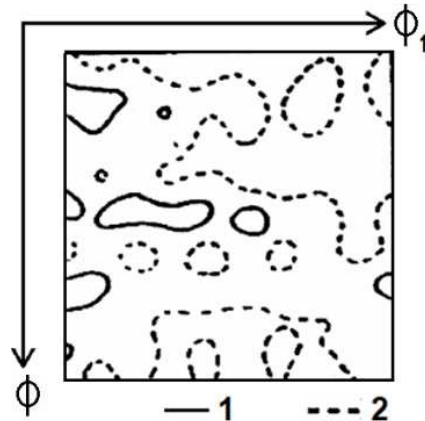


Figure 9: Pictorial Representation of Orientation Distribution Function Components of 0.07% Cu EDD steel in $\Phi_2=45^\circ$ Sections. Though not Complete, it is Most Concise

REFERENCES

1. Kanniraj, A., & Padmanabhan, K.A. (1998). Formability of Metastable Austenitic Stainless Steel Sheets: I Experimental. *Transactions of the Indian Institute of Metals*, 51, 201- 215.
2. Singh, R.K.P., Padmanabhan, K.A., & Mishra, S. (1994). Effect of composition and rolling parameters on the physical and metallurgical properties of EDD low carbon AK steel sheets. *Manufacturing Science and Engineering*, ASME, 2, 583-597
3. Kanniraj, A. (2010). Calculation of Lankford coefficient from orientation distribution function and computational numerical mathematical modelling of forming limit diagram using Marciniak-Kuczynski hypothesis of geometric instability. *Indian Journal of Engineering & Materials Sciences*, 17, 256-264
4. Zhang, R., Shao, Z., & Lin, J. (2018). A review on modelling techniques for formability prediction of sheet metal forming. *International Journal of Lightweight Materials and Manufacture*, 1, 115-125
5. Takalkar, A., Rao, J.M.K., & Babu, M.C.L. (2015). Numerical simulation for predicting failure in deep drawing process using forming limit diagram (FLD). *International Journal of Advances in Mechanical and Civil Engineering*, 2(4), 11-15
6. Reddy, C. (2017). Experimental and numerical studies on formability of stainless steel 304 in incremental sheet metal forming of elliptical cups. *International Journal of Scientific & Engineering Research*, 8(1), 2017, 971-976
7. Hora, P., & Volk, W. (2012). *Proceedings of Advanced Failure Prediction Methods in Sheet Metal Forming*, Zurich :Institute of Virtual Manufacturing
8. Srinivasan, S., Krishna, G., Shenoy, S.K., Singh, S.K., & Gupta, A.K. (2014). Prediction of Forming Limit Curves for Extra Deep Drawn (EDD) steel using Marciniak and Kuczynski (MK) model. *Manufacturing Technology, Design and Research Conference*, December 12–14, IIT Guwahati, India
9. Hounjaloune, S., Hiroyoshi, N., & Ito, M. Effect Of Reaction Temperature On Schwertmannite Synthesis, From Simulated Copper Heap Leach Solutions.
10. Tisza, M., & Czinege, I. (2018). Comparative study of the application of steels and aluminium in lightweight production of automotive parts. *International Journal of Lightweight Materials and Manufacture*, 1, 229-238
11. Stoughton, T.B., & Yoon, J.W. (2012). Path independent forming limits in strain and stress spaces, *International Journal of Solids and Structures*, 49, 3616–3625

12. Sivam, S.P.S.S., Gopal, M., Venkatasamy, S., & S. Singh (2015). Application of forming limit diagram and yield surface diagram to study anisotropic mechanical properties of annealed and unannealed SRPC 440E steels. *Journal of Chemical and Pharmaceutical Sciences*, 9, 15- 22
13. Fahad, K. K. Levels Of Heavy Metals (Cadmium, Copper And Zinc) In The Tissues Of Four Fish Species Of The Euphrates river; Thiqr, Iraq.
14. Goud, R.R., Prasad, K.E., &Singh, S.K.(2014). Formability limit diagrams of extra-deep-drawing steel at elevated temperatures, *Procedia Materials Science*, 6, 123 – 128
15. Qashqaei, A., & Asl, R. G. (2015). Numerical Modeling and Simulation Of Copper Oxide Nanofluids Used In Compact Heat Exchangers. *International Journal of Mechanical Engineering*, 4(2), 1-8.
16. Kanniraj, A. (2008).Room temperature formability of AISI 304 stainless steel sheet. *Manufacturing Technology Today Journal*, 7(4), 56-62